Mon. Not. R. Astron. Soc. **000**, 1–?? (2012) Printed 8 February 2013 (MN LaTeX style file v2.2)

arXiv:1302.1778v1 [astro-ph.CO] 7 Feb 2013

Interaction between collisionless galactic discs and nonaxissymmetric dark matter haloes

A.V. Khoperskov,[1] S.A. Khoperskov,[2,3] A.V. Zasov,[3] D.V. Bizyaev,[3,4] S.S. Khrapov[1]
[1] *Volgograd State University, Universitetsky pr., 100, 400062, Volgograd, Russia*
[2] *Institute of Astronomy Russian Academy of Sciences, Pyatnitskaya st., 48, 119017, Moscow, Russia*
[3] *Sternberg Astronomical Institute, Moscow M.V. Lomonosov State University, Universitetskij pr., 13, 119992, Moscow, Russia*
[4] *New Mexico State University and Apache Point Observatory, P.O. Box 59, Sunspot, NM 88349, USA*

ABSTRACT

Using N-body simulations ($N \sim 10^6 - 10^7$), we examine how a non-axisymmetric dark halo affects the dynamical evolution of the structure in collisionless (stellar) discs. We demonstrate how the model parameters such as mass of the halo, initial conditions in the disc and the halo axes ratio affect morphology and kinematics of the stellar discs. We show that a non-axisymmetric halo can generate a large-scale spiral density pattern in the embedded stellar disc. The pattern is observed in the disc for many periods of its revolution, even if the disc is gravitationally over-stable. The growth of the spiral arms is not accompanied by significant dynamical heating of the disc, irrelevant to its initial parameters. We also investigate transformation of the dark halo's shape driven by the long-lived spiral pattern in the disc . We show that the analysis of the velocity field in the stellar disc and in the spiral pattern gives us a possibility to figure out the spatial orientation of the triaxial-shaped dark halo and to measure the triaxiality.

Key words: Galaxies: evolution; galaxies: haloes; galaxies: kinematics and dynamics; galaxies: spiral

1 INTRODUCTION

Both dynamic models of real galaxies and cosmological simulations give a strong evidence that the stellar discs of spiral galaxies are embedded into massive dark haloes. The halo mass and its influence on the disc evolution is the matter of debates. Among the different ways to put constraints on the halo mass it is worth mention the use of gravitational stability criteria in the disc's plane (Safronov 1960; Toomre 1964; Lynden-Bell and Ostriker 1967; Khoperskov et al. 2003; Zasov et al. 2004), a condition of stellar disc stability to bending perturbations (Zasov et al. 1991; Sotnikova et al. 2005; Khoperskov et al. 2010), simulation of polar rings (Whitmore et al. 1987; Sackett and Sparke 1990; Reshetnikov and Sotnikova 2000; Iodice et al. 2003), and the gravitational lensing (Koopmans et al. 1998; Maller et al. 2000; Oguri et al. 2003).

Morphology of galactic spiral patterns also indicates significant amount of the dark matter within the optical radius (Athanasoula et al. 1987; Korchagin et al. 2000; Griv and Gedalin 2004). Estimates of the dark mass contribution can also be obtained from the vertical structure of stellar discs analysis (e.g. Bahcall (1984); Zasov et al. (1991); Bizyaev and Mitronova (2002); Zasov and Bizyaev (2002); Korchagin et al. (2003); Bizyaev and Mitronova (2009); Just and Jahrei (2010); Garbari et al. (2011)). Maximum disc models suggest that $M_h/(M_d + M_b) \simeq 0.5 - 1$, where M_h is the halo mass within the optical radius, M_b is the mass of stellar bulge, M_d is the mass of stellar disc (Bottema 1993). Note that some galactic discs (especially low luminous ones) are less massive than that required by the maximum disc assumption (Zasov et al. (2004); Bershady et al. (2011); Westfall (2011); Saburova and Zasov (2012)). At any case, one may conclude that in most galaxies (at least of normal surface brightness) masses M_h and M_d are comparable within the optical borders.

Modern cosmological experiments suggest a triaxial distribution of the dark matter in the haloes (e.g. Zentner et al. (2005); Kuhlen et al. (2007), Muoz-Cuartas et al. (2011), Klypin et al. (2011), and references therein). Intriguing problem is a possibility to explain the generation and support for the long-lived and extended spiral structure in the stellar discs by triaxial potential of the dark halo. True mechanism of the formation of the spiral structure is still a subject of discussions. Although a bar or a close satellite may induce the spiral density wave, these events provide a relatively short term support. In contrast, the dark halo can keep its triaxiality and support the spiral structure over much longer time scale. The problem is to estimate whether the existing

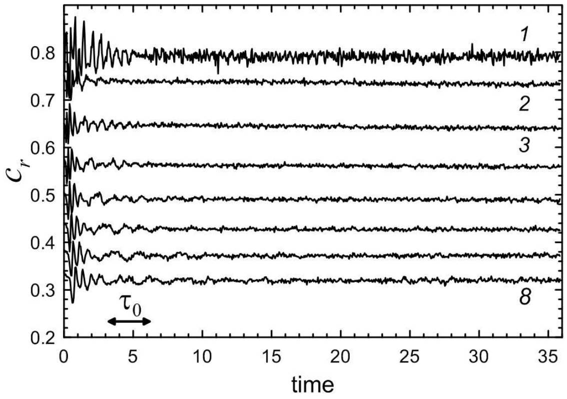

Figure 1. Evolution of the stellar velocity dispersion c_r at different radii r in a model with spherically symmetric halo. The curve *1* demonstrates the central zone of the disc, the curve *8* – the periphery of the disc. The arrow indicates the time interval corresponding to one period of rotation τ_0 at the disc's periphery.

deviation from the axial symmetry is *quantitatively* enough to support the spiral pattern in collisionless gravitationally stable discs.

Usually the distribution of the volume density in the halo is approximated as follows:

$$\varrho_h(x, y, z) = \varrho_h(\xi)\,, \quad \xi \equiv \sqrt{\frac{x^2}{a^2} + \frac{y^2}{b^2} + \frac{z^2}{c^2}}\,, \qquad (1)$$

where the $a = b = c$ case corresponds to the spherical symmetry in the density distribution. The model with $a = b \neq c$ corresponds to an axisymmetric halo coplanar with the stellar disc. Note that in this labeling convention, the relative ordering of a, b, and c is unconstrained. The ratios $q = b/a$, $s = c/a$ describe the deviation of the density profiles front the spherical symmetry. For simplicity, our further consideration of the dark matter (DM) haloes assumes that $a \geqslant b$ and $c = a$, where a and b are the halo major and minor axes in the disc plane.

Cosmological N-body simulations show that the triaxiality parameters s and q depend on the halo mass and distance to the centre (Bailin and Steinmetz 2005; Hayashi et al. 2007; Widrow 2008). Simulations conducted with a large number of particles (as the Via Lactea with $N = (1 - 2.3) \cdot 10^8$, Diemand, Kuhlen and Madau (2007); Kuhlen et al. (2007); Debattista et al. (2008); Diemand and Moore (2009)) reveal that the dark haloes are more asymmetric at their central regions than at the periphery where the ratios b/a and c/a are close to to unit. For the topic of this paper the most important parameter of the halo's shape is the axes ratio q.

Observing constraints on the dark halo geometrical parameters come from studies of globular clusters, variable stars (such as RR Lyrae), blue horizontal branch stars, low-metallicity giants, red giants, Cepheids (W Vir type) and F-dwarfs (Keller et al. 2008). Anisotropy of the velocity dispersion of objects in the stellar halo of our Galaxy indicates an asymmetric distribution of DM (Morrison et al. 2009). Stellar haloes in other spiral galaxies also demonstrate significant deviation from spherical symmetry in the haloes: $c/a \sim 0.3$ is suggested by Cooper et al. (2010). According to the Sloan Digital Sky Survey (SDSS) and Sloan Extension for Galactic Understanding and Exploration results, our galactic spheroid has a triaxial shape with $s = 0.63$, $q = 0.75$ (Newberg et al. 2007).

The polar ring galaxies are unique objects for investigation of the DM halo shape (Combes 2006). Whitmore et al. (1987) analysed the polar ring kinematics in several galaxies and found significant deviation of the DM distribution from the spherical shape: $c/a \sim 0.5$ (Sackett and Pogge 1995), $c/a \sim 0.3 - 0.4$ (Sackett et al. 1994). A prolate shape of the dark matter haloes was inferred by Iodice et al. (2003) based on the analysis of location of the polar ring galaxies on the Tully-Fisher diagram.

Dynamics of decaying satellites also helps to constrain the dark halo properties, such as its shape, orientation, mass distribution (Ibata et al. 2001b; Helmi 2004; Fellhauer et al. 2006). According to Sesar et al. (2011), SDSS data suggest that the Milky Way's dark halo is oblate ($s = 0.7$) and non-axisymmetric in the disc plane ($q = 0.98$) within 28 kpc of the centre.

An assumption of the axissymmetric potential for the Milky Way halo applied to the Sgr dSph tidal stream yields controversial results: while the leading arm of the stream requires an oblate halo, the radial velocity distribution of stars in the arm agrees better with a prolate halo (Vivas et al. 2005). Note that the introduction of a triaxial potential helps to resolve this ambiguity (Law et al. 2009).

Statistical analysis of shapes of the spiral galaxies also reveals some deviation from the disc axial symmetry, which in turn may evidence the halo triaxiality. According to Ryden (2006), the disc ellipticity is $0.02 - 0.3$ in the K_s photometric band. The ellipticity varies in dependence of the photometric band and of the galaxy morphological type (Ryden 2006).

Despite direct and non-direct evidences of the halo triaxiality mentioned above, its shape and ellipticity in specific galaxies remains poorly known. Understanding of the role that the asymmetry of the halo potential can play in dynamical evolution of stellar discs in galaxies remains incomplete. El-Zant and Habler (1998); Ideta and Hozumi (2009); Tutukov and Fedorova (2006); Berentzen and Shlosman (2006); Hayashi and Navarro (2006); Hayashi et al. (2007) studied different aspects of how a non-axisymmetric gravitational potential affects the galactic disc's dynamics. The triaxial halo allows to explain the observed shape of rotation curves in low surface brightness (LSB) galaxies (Hayashi and Navarro 2006; Widrow 2008).

Galaxies with warped discs were successfully reproduced within the models with triaxial dark matter (DM) halo (Dubinski and Chakrabarty 2009; Roskar et al. 2010). The effects of the bar response to the triaxial halo perturbations and bar dissolution in prolate halo were studied by Machado and Athanassoula (2010) and Kazantzidis et al. (2010). Numerous N-body simulations are usually used to study the formation and evolution of stellar bars embedded in triaxial dark matter haloes (Athanasoula 2002; Berentzen et al. 2006; Dubinski et al. 2009). The triaxial halo can destroy stellar bars due to the angular momentum exchange (Berentzen and Shlosman 2006). The decreasing of the bar pattern speed was demonstrated in models with triaxial dark matter halo (Ceverino and Klypin 2007).

Bekki and Freeman (2002) explained the spiral structure extended far beyond optical limits in a blue compact

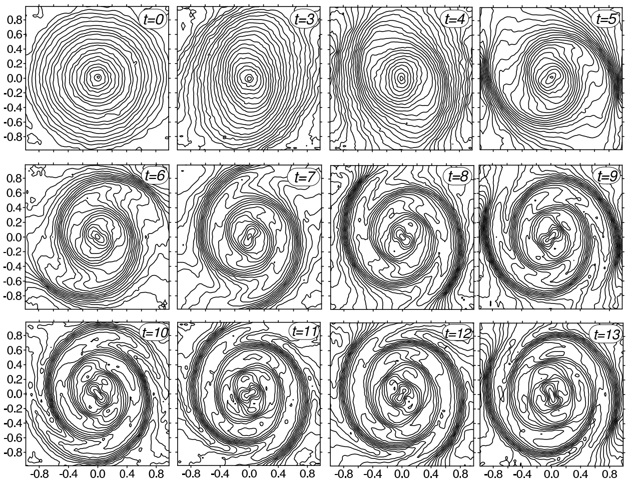

Figure 2. The surface density isolines $\sigma(r,\varphi)$ at different time t in the model with $\varepsilon = 0.1$ (σ is shown in the log scale). One period of rotation at the disc's periphery corresponds to about 3 our dimensionless units.

dwarf galaxy NGC 2915 by the presence of a triaxial dark halo. Masset and Bureau (2003) modeled the spiral structure in the outer region of the gaseous disc of NGC 2915 generated by a triaxial dark matter potential. The main result of these papers is that triaxial DM halo is able to produce a two-arm spiral pattern in external regions beyond the optical radius. Tinker and Ryden (2002) investigated effects of rotating triaxial haloes in the disc galaxies using N-body simulations with the rigid halo potential and found that the average pitch angle of the spiral structure strongly anticorrelates with the total mass of the system (disc+halo). Dubinski and Chakrabarty (2009) applied N-body simulations to demonstrate the formation of warps and spirals in isolated discs embedded in triaxial haloes. They showed that the spiral pattern may emerge in gravitational stable stellar disc through interactions with a non-axisymmetric halo. Note that the evolution of the grand design spiral structure in stellar discs embedded in the triaxial dark matter haloes remains poorly studied.

In our previous paper (Khoperskov et al. 2012) we studied the dynamics of a gaseous galactic disc in a non-axisymmetric gravitational potential in general. In the present paper we perform N-body modelling (with $N \sim 10^6 - 10^7$) of stellar collisionless discs embedded in a non-axisymmetric dark halo with focusing on the formation of the spiral pattern, its morphology and kinematics. In Section 2 we describe our modelling technique and the initial conditions in the our galactic discs. The spiral structure formation and the kinematics of the density waves are analysed in Section 3. Discussion and main conclusions are given in Sections 4 and 5, respectively.

2 MODELLING COLLISIONLESS STELLAR DISCS

Throughout this paper we study the dynamics of the galactic discs in the frames of a self-consistent N-body problem by solving the motion equations for equal mass test particles:

$$\frac{d^2\mathbf{r}_j}{dt^2} = -m\sum_{\substack{i=1\\ i\neq j}}^{N}\frac{(\mathbf{r}_j-\mathbf{r}_i)}{|\mathbf{r}_j-\mathbf{r}_i|^3}-\frac{\partial\Psi_b}{\partial\mathbf{r}_j}-\frac{\partial\Psi_h}{\partial\mathbf{r}_j}\,, \quad j=1,2,...,N\,, \tag{2}$$

here $\mathbf{r}_j = \{x,y,z\}$ is the coordinate vector of j -th particle, M_d is the total stellar disc mass, $\Psi_b(x,y,z)$ is the bulge potential, $\Psi_h(x,y,z,t)$ is the halo potential and $m = M_d/N$ is the mass of a test particle.

The force of gravity in the disc is determined by the summation over all particles in Equation (2) and calculations via the TreeCode Top Down algorithm (Barnes and Hut 1986). Initial distribution functions in the equilibrium stellar disc are described in detail in our previous papers (Khoperskov et al. 2003, 2010). The schemes of the 2nd and 4th orders we apply provide a good accuracy of integration of Equations (2).

We introduce the following dimensionless model units: Our spatial distance unit is assumed to be 10 kpc, the gravitational constant is chosen to be $G = 1$, the time unit is 91 Myr, the velocity is expressed in the units of 110 km s^{-1}. Assumptions $G = 1$, $V = 1$ lead to the total mass of model galaxy equal to about $10^{11} M_\odot$ within $R = 1$.

The number of particles in our models is $N = (1-10)\cdot 10^6$. The potential for i-th particle at j-th point is $\Psi_{ij} = -m/\sqrt{r_{ij}^2 + r_c^2}$, where the cut off radius is $r_c \leqslant 10^{-3}$ (which corresponds to $\leqslant 10$ pc). The opening angle parameter Θ is assumed to be $0.1-0.5$, although we did not find significant variations of the results between models with different Θ. The results presented in this paper were obtained assuming $\Theta = 0.1$, if alternative value is not specified. This values of r_c and Θ determine the accuracy of the calculations. The integration step is chosen to be $2\cdot 10^{-3}$, which approximately corresponds to $2\cdot 10^5$ yr.

Basic model parameters are constrained in the range suggested by observations as follows:

- Relative dark halo mass $1 \leqslant \mu = M_h/M_d \leqslant 4$ within the limits of the stellar disc $R = 4r_d = 1$, where r_d is the radial scalelength of the disc.
- $\mu_b = M_b/M_d = 0 - 0.3$ is the relative stellar mass of the bulge with scalelength $r_b = 0.1 - 0.3$.
- $\tau_0 \approx 3$ is the period of rotation at the periphery of the disc.
- Nonaxissymmetric halo parameter $\varepsilon = 1 - b/a = 0 - 0.25$ in the disc plane [1].
- $\Omega_h = 0 - 0.3$ is the angular rotation velocity of the halo. The halo corotation radius is located far outside the stellar disc ($\Omega_h = 0.3$ or about 3 km s^{-1} kpc^{-1}).
- $\tau_h = 0 - 20$ is the time scale of variation of the non-axisymmetry parameter from 0 to ε.

---

[1] It should be emphasised that the value $\varepsilon = 1 - b/a$ calculated for the dark halo volume density distribution differs from that for the gravitational potential ε_Ψ. Approximately, $\varepsilon_\Psi \simeq 3\varepsilon$ (Binney and Tremaine 2008).

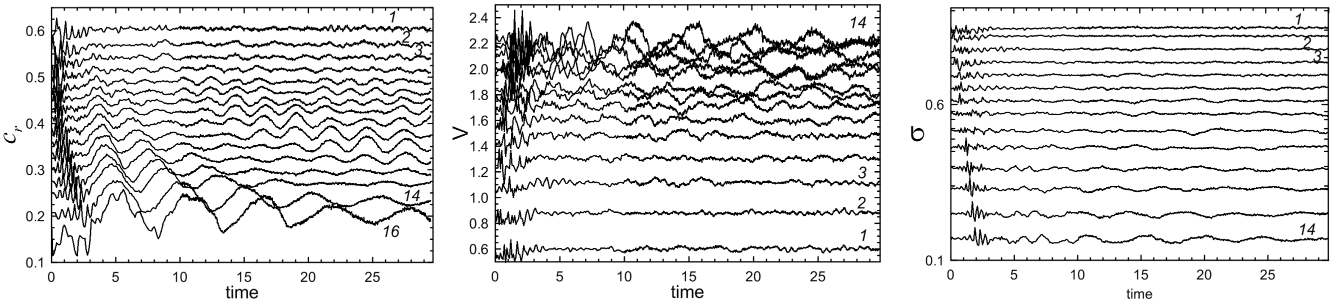

Figure 3. Evolution of the disc parameters averaged over the azimuthal angle at various distances from the centre (curve number increases from the centre towards the periphery). Strong fluctuations at the beginning of the experiment ($t < 5$) are due to the deviation from precise balance at the initial moment.

We assume the exponential surface density distribution in the disc as an initial condition: $\sigma(r) = \sigma_0 \exp(-r/r_d)$, where $r_d = 0.25$ of dimensionless distance units is the radial scale length in the disc. At the initial stage, all stellar disc particles are situated within the radius $r \leqslant 5r_d = 1.25$. We assume a flat rotation curve with the maximum velocity $V_{\max} \simeq 2$ in dimensionless units, which corresponds to the rotation period of $\tau_d \simeq 3$ at the disc's periphery.

Following Begeman et al. (1991), we use a pseudo-isothermal model of the density distribution in the halo:

$$\varrho_h(r) = \frac{\varrho_{h0}}{1+(r/a)^2}\,. \qquad (3)$$

This distribution of the dark mass provides a constant circular velocity V_c for $r \gg a$. The gravitational potential can be written

$$\Psi_h(x,y,z) = 4\pi G \varrho_{h0} a^2 \cdot \left\{ \ln(\xi) + \frac{\mathrm{arctg}(\xi)}{\xi} + \frac{1}{2}\ln\frac{1+\xi^2}{\xi^2} \right\} \qquad (4)$$

(Khoperskov et al. 2012), which corresponds to the density law (3) for the case of $a = b = c$.

Note that the cosmological simulations predict that virialised dark matter haloes should have a universal density profile. For a spherically averaged density distribution it can be written (Navarro et al. 1997):

$$\varrho_h(r) = \frac{\varrho_{h1}}{(r/a)\left(1+(r/a)\right)^2}\,. \qquad (5)$$

Its distinctive feature is the inner density cusp, which however may be dissolved due to its interaction with baryonic matter in the central region of galaxies (see f.e. Gustafsson et al. (2006); Maccio et al. (2012); Khoperskov et al. (2012)). Moreover, inevitable singularity emerges at $r = 0$ in the case of transformation from a spherical NFW profile to the triaxial shape. Another widely used dark matter density distribution is Burkert's profile (Burkert 1995), which usually fits observing data very well (Gentile et al. 2005). It is very close to the NFW profile: it has a cored density distribution in the inner part ($r < a$). Several more halo density profiles were introduced, such as exponential profile Fux (1997) and Einasto profile (Einasto 1965). All density distribution functions mentioned above (except (5)) allow generalization of the spherical dark matter distribution shape to the triaxial case using the formal replacement $r \to \xi$ (see eq. 1). Note however, that the choice of the accepted law for $\varrho_h(r)$ makes only a small effect on the results described below.

Rotation pattern in the dark haloes predicted by ΛCDM cosmological models is similar to that in giant elliptical galaxies, where the kinetic energy of the rotation is much smaller than that in the stellar chaotic motions. The origin and properties of angular momentum of DM haloes were investigated by Vitvitska et al. (2002); Maccio et al. (2007); Bett et al (2007). For the disc galaxies cosmological simulations suggest slow rotation of their dark matter haloes within R_{opt}. The rotation (tumbling) of the overall shape of the halo in ΛCDM simulations was discussed by Bailin and Steinmetz (2004); Bryan and Cress (2007). Authors conclude that the tumbling rates of the haloes are less than one km s^{-1} kpc^{-1}. Evidently, a disc subsystem rotates much faster than a halo. Hereafter we use a non-rotating or slow rigidly rotating model halo with the angular velocity Ω_h, which places the corotation radius at the disc's periphery $\Omega_h \lesssim V_{\max}/R_{opt}$. Our principal results are shown for the case of rigid DM halo, while the situation with the live halo is considered in Section 3.4.

3 DISC DYNAMICS: PROPERTIES OF THE SPIRAL STRUCTURE

Propagation of the density waves of gravitational nature in a self-gravitating stellar disc requires that the stellar velocity dispersion were close to the stability condition $Q_T \leqslant 2$ (or $Q_T \leqslant 3$ at the periphery of the disc, see Khoperskov et al. (2003)), where Q_T is the Toomre stability parameter (Toomre 1964). The case $Q_T = 1$ is unstable due to non-radial perturbations. In the following section we consider gravitationally stable discs ($Q_T \sim 2-4$ at $r \sim (1-2)\cdot r_d$) and study the pure effects from the non-axisymmetric dark matter distribution. We also compare the properties of the spiral pattern generated by triaxial haloes in the cases of stable and unstable discs (see Section 3.3).

3.1 Dynamically stable stellar discs

The initial distributions of the radial c_r, azimuthal c_ϕ and vertical velocities dispersions c_z are chosen to be high enough to prevent the disc gravitational instability, which is able to generate spiral waves in the initially axisymmetric model by its own. The stellar velocity dispersion should be high enough to support the gravitational stability against

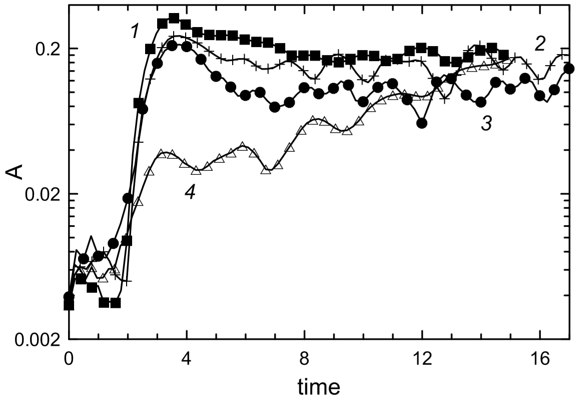

Figure 4. Amplitudes of the Fourier harmonics for $m = 2$ mode for the entire disc in different models: *1* : $\mu = 4$, *2* : $\mu = 3$, *3*: $\mu = 2$, *4*: $\mu = 1$ ($\varepsilon = 0.15$, $r_b = 0.3$ for all models).

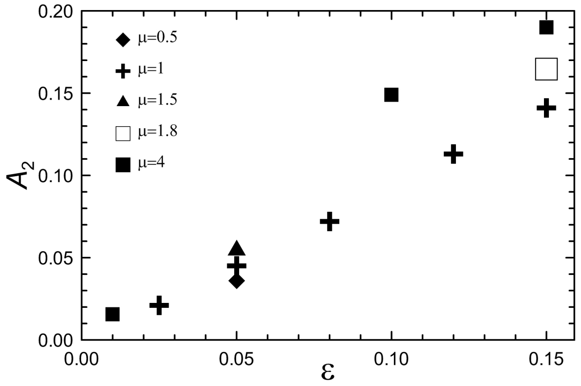

Figure 5. Mean amplitude of the time-averaged Fourier harmonics for the entire disc in the two-arm mode as a function of the parameter ε.

perturbations in the disc plane and against the bending instability (Khoperskov et al. 2010). An iterative procedure is applied for making marginally stable 3-D stellar discs as described by Khoperskov et al. (2003).

First, we tested the disc's stability in the potential of the spherical halo. We assureed that the initial disc parameters ($c_r(r)$, $c_\varphi(r)$, $c_z(r)$, rotation velocity $V(r)$, surface density $\sigma(r)$, and the disc vertical scale $h(r)$) do not change significantly during several revolutions of the disc. As an example, figure 1 illustrates the temporal variation of the $c_r(r)$. Collisionless stellar disc in this model does not undergo any dynamic heating neither to binary particle interactions nor due to collective processes. Under the chosen conditions the disc remains axisymmetric during dozens revolutions (which corresponds to a few billion years).

3.2 Generation of the spiral structure in the stellar disc

Our simulations started from the spherical halo and axisymmetric stellar disc, then we slowly and adiabaticically (over time scale $\tau_h \sim 3$) increased the halo's non-axisymmetric parameter ε.

We performed about 30 modelling runs with different sets of initial model parameters mentioned above. It is evident that in all models with $\varepsilon > 0.05$ the presence of the non-axisymmetric dark halo excites the formation of a two-arm spiral pattern in the stellar disc. In figure 2 we show snapshots of the typical evolution of the surface density in the model with $\varepsilon = 0.2$. Within 1-2 periods of rotation τ_0, a two-armed spiral structure forms in the initially axisymmetric exponential disc. A nested Θ-like structures and a central bar can be identified in the inner disc region ($r \leqslant 0.2 \leqslant r_d = 0.25$). The rigid triaxial halo models (models without the disc feedback to the halo) generate a long lasting global spiral pattern that extends from the centre to the disc periphery. It is important to note that interactions between the disc and non-axisymmetric dark halo's potential do not introduce any significant systematic variations to the azimuthally-averaged disc parameters.

Evolution of $c_r(r)$, $V(r)$ and $\sigma(r)$ is shown in figure 3. Note that the centre of the disc (curves 1 and 2) remains unperturbed over the course of the simulations, whereas quasi-periodic radial oscillations can be observed, especially in the outer part of the disc. In contrast to the global gravitational stochastic spiral structure that develops in the slightly unstable discs (De Simone et al. 2004), here the heating of the stellar disc is insignificant (except for the short initial stage of the experiment).

The model parameters μ, μ_b, r_b and τ_h significantly affect the growth increment of the spiral structure. The amplitude of the stellar density wave at early stages in the simulations is primarily determined by the relative halo mass parameter μ (see figure 4). However, after several τ_0, two-arm spirals reach the similar amplitudes at a fixed value of ε, independently of μ. Our modelling demonstrates the dependence of the eventual amplitude A_2 of the spiral waves on the triaxiality parameter ε for the spiral mode $m = 2$ (see figure 5). It seems that ε is a crucial parameter, which defines the properties of the strength of the spiral structure as a whole. Despite the fact that the growth rate of the spiral waves depends on the relative mass of the halo (see figure 4), the final amplitude of the waves is determined by the non-axisymmetric parameter ε (see figure 5).

There are two distinctive properties of the spiral structure generated by the triaxial halo. First, the spirals are generated in a sufficiently hot (i.e. gravitationally stable) disc with the Toomre parameter $Q_T \sim 2 - 4$, in contrast to the standard density waves theory. Therefore, this mechanism can produce spirals even in the over-stable stellar discs, e.g. in the outer regions of galaxies far beyond their optical size limits, where the disc surface density is much lower than the gravitational stability threshold. Second, the formation of the spiral structure leads to a weak stellar disc warming-up during the initial stage of the spiral pattern development, and after that the velocity dispersion components only slightly increases even in the case of high amplitude spiral waves (figure 3). These properties are significantly different from those seen in N-body simulations of gravitationally unstable discs, in which the development of the gravitational instability is accompanied by significant growth of the velocity dispersion during one period of rotation. It should be noted that a slight disc heating for large amplitude waves that we observe in the our modelling may be a result of limited accuracy in the numerical solution of the motion equations (2). Indeed, we found that the disc heating decreases with the increasing of the number of test particles. The heating up effect may also be attributed to the lack of perfect disc equilibrium at the beginning of the simulations. The final conclusion about the low disc heating requires modelling with higher spatial resolution.

3.3 Simulations with different stellar disc initial state

While we started simulations with the initially stable disc in the previous section, we should consider whether the initial gravitational instability of the disc can qualitatively change the results of section 3.2. To reveal the effect of self-gravity we have performed simulations for initially unstable disc by assuming the relative halo mass $M_t/M_d = 1$ and $Q_t = 1$. We started with the axisymmetric halo to be sure that the evolution of the disc and spiral structure is fully determined by the global gravitational instability of the entire disc, and that the formation of the spiral waves is accompanied by the disc heating up to the marginal stability condition (see Figure 6). After that we ran another simulation with the same initial conditions, but assuming the halo with $\epsilon = 0.1$. Relatively low halo mass led to slower growth of the wave amplitude than that shown in Figure 4 for $\mu = 1$. Curiously, the final amplitude of the spiral waves is practically the same independently on the mechanism of their generation (either non-axisymmetric halo +gravitational instability, or pure gravitational instability). A general character of the evolution of the velocity dispersion is also very similar in both models. It confirms that the non-axisymmetric halo does not contribute essentually to the eventual disc heating.

To analyze the direct role of a triaxial halo and to separate it from effects of the disc initial state, below we compare different numerical models of evolution of gravitationally stable stellar discs in the halo field. It was assumed that the disc always remains in a quasi-equilibrium state even it is non-axisymmetric, since the halo shape changes slowly and adiabatically in our models. Model (a) is a "reference" model for the initially round-shaped disc described in Section 3.2. In model (b) we introduce a very large timescale for the halo triaxiality growth ($\tau_h = 15$) for initially round disc to be sure that the disc has enough time to follow the slowly changing halo potential. In our third model (c) we use the initially elliptical disc with the same spatial major axis orientation as for the non-axisymmetric halo. In our last model (d) we took the results of long-time evolution of a "reference" model of round disc in the non-axisymmetric halo at $t = 20$. After that the spiral structure was radially smoothed (which introduced slight ellipticity to the disc), and next simulation was started from this equilibrated, spiral-free initial state.

Results of modelling are shown in Figure 7. In all four models the spiral structure emerges. The main difference between the models is observed at the central part of the disc. In models (a) and (b) a Θ-like structure forms. In the model (c) of initially elliptical disc a large bar was formed, and beyond the bar there is a tightly wound spiral structure. In the case (d) there is a small bar and very even spiral arms. Formation of a bar in the potential of triaxial DM halo links our models with those developed by Berentzen et al. (2006), where the bar generation and bar-halo interaction are also described. It is essential that our models demonstrate the emergence of the spiral arms in the very outer regions of the disc driven by the halo triaxiality, independently of the disc gravitational stability and its initial shape.

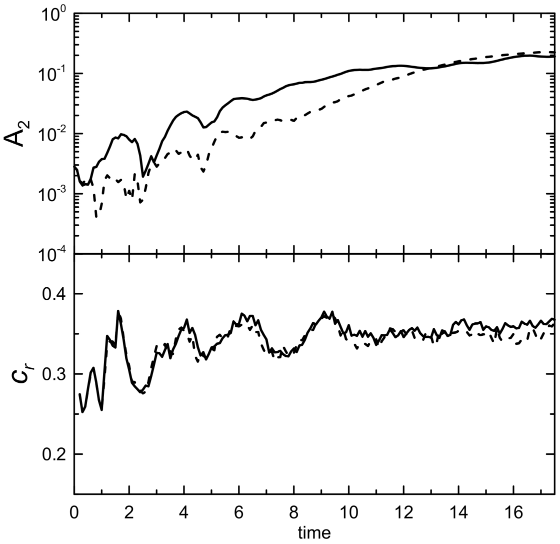

Figure 6. Top panel: evolution of the Fourier harmonic $m = 2$ in a gravitationally unstable disc ($Q_T = 1$) embedded in a non-axisymmetric halo $\varepsilon = 0.1$ (solid line) and in a symmetric halo (dashed line). Bottom panel: evolution of the velocity dispersion in the same two models at the radius of $r = 0.5$.

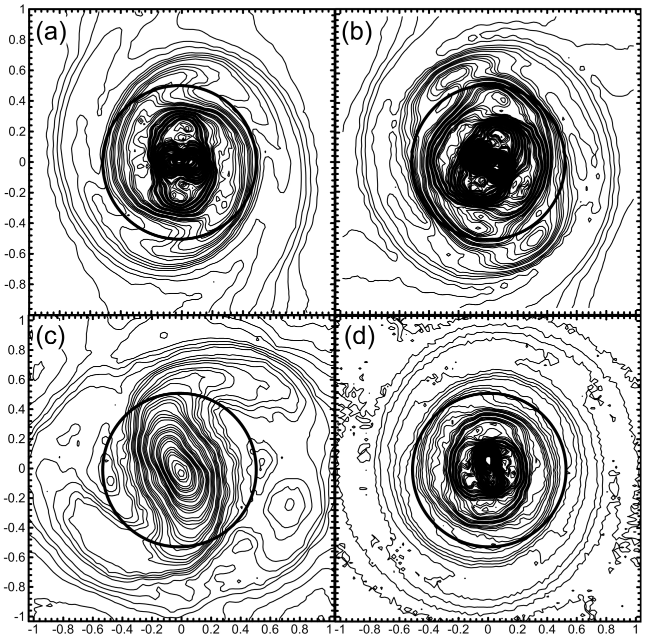

Figure 7. Disc surface density at $t = 8$ in models with different initial state of the stellar disc for the non-axisymmetrical halo with $\varepsilon = 0.1$: (a) the reference model of the symmetric disc; (b) evolution with long term quasi adiabatic growth of ε with $\tau_h = 20$; (c) the model with a non-axisymmetric disc; (d) the model started with a radially smoothed disc made with those from the model (a) after $t = 20$ evolution.

To analyze the properties of the spiral structure without considering the central disc regions, we considered the evolution of the Fourier harmonics and velocity dispersion beyond the radius $r = 0.5$ (the solid circle in Figure 7). De-

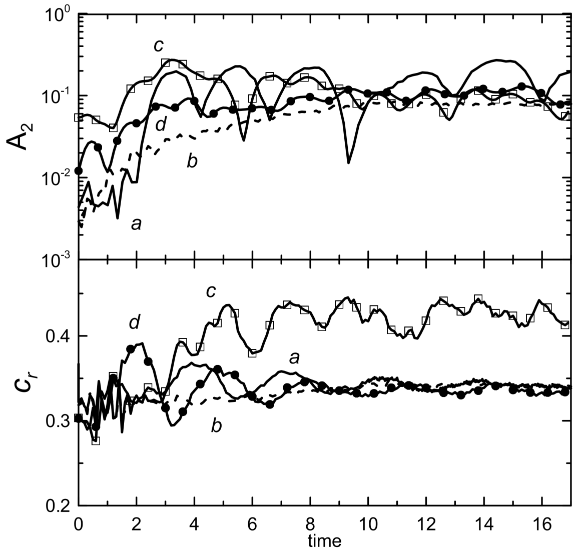

Figure 8. Analysis of the spiral arms in different models beyond $r = 0.5$ — the designations are kept the same as in figure 3.3. Top panel: evolution of the Fourier harmonic $m = 2$. Bottom panel: evolution of the velocity dispersion.

spite the difference in the disc initial state, the amplitude and its time-dependent evolution are rather similar (see Figure 8, top panel). The final amplitude of the spiral waves is about 10% in all cases. The initial values of the Fourier harmonics $m = 2$ in (c) and (d) models are large because of the initial ellipticity. The model (b) with a long timescale of the shape formation of adiabatic halo shape transformation reveals a slow quasi-steady increasing of the spiral wave amplitude, which follows the slow growth of the halo triaxiality. These numerical experiments confirm that formation of the spiral structure in the models is entirely due to interaction of the disc with the non-axisymmetric halo. After the spirals have formed, there is no significant dynamical heating introduced to the disc (see bottom panel in Figure 8). Some initial growth of the velocity dispersion observed in the model (c) is caused by the relaxation processes in the elliptical-shaped disc while it transits to another (also elliptical) disc state due to interaction with equally oriented halo. After this transition has finished the disc heating is ceases.

3.4 Kinematics of the spiral structure

The non-stationary evolution of the spiral waves is characterised by quasi-periodic oscillations that are caused by the radial propagation of spiral waves (figure 3). The spiral wave pattern rotates with the angular velocity Ω_p, which slightly changes with time. Figure 9 shows the evolution of the wave amplitude at different radii. Estimation of the phase shift along the radius enables us to find the pitch angle of the spiral pattern, which ranges from 5° to 30°. For illustration, we assume it to be $\sim 12°$ in our model with $\varepsilon = 0.1$. In our simulations, the pitch angle is a function of radius: it grow from the centre to the periphery in the galactic disc, so the spiral arms become more open. This radial dependence may be used for the revealing of the halo non-axisymetry signature in the real galaxies.

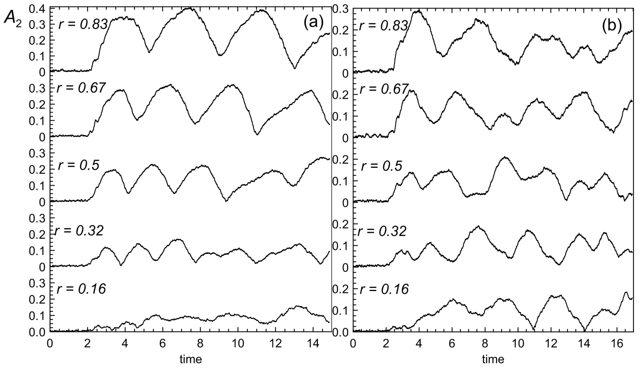

Figure 9. Evolution of the amplitude of the Fourier harmonic $m = 2$ in the surface density distribution at various distances from the centre of the disc r as a function of time: a) $\mu = 4$ and $a = 0.3$; b) $\mu = 1.8$ and $a = 0.3$.

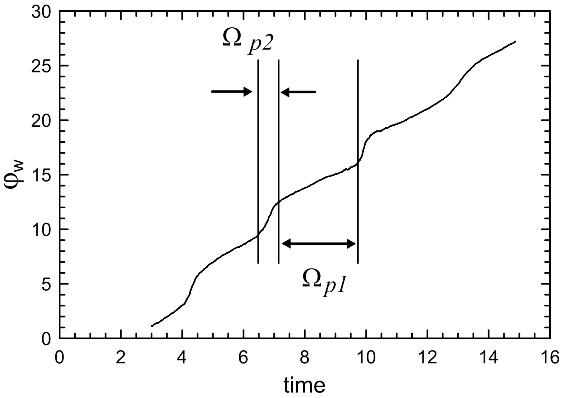

Figure 10. The change of the wave phase $\varphi_W(t)$ at fixed radius $r = 0.67$ (see figure 9a). There are two stages distinguished by their different angular velocities $\Omega_p = d\varphi_W/dt$: slow rotation with Ω_{p1} and a short phase of fast rotation with $\Omega_{p2} > \Omega_{p1}$

A distinctive feature that we observe in our modelling is that the spiral pattern does not show a rigid-body rotation. Instead, at any radial distance in our models, its possesses a two-pattern angular velocity, which switches from Ω_{p1} to Ω_{p2} and back (see figure 10) twice during the orbital period. Most of the time the wave rotates more slowly (angular velocity Ω_{p1}), which corresponds to the case when the corotation radius r_{c1} locates at the periphery of the disc or beyond it. When the wave passes through the dark halo potential well, its angular rotation rises to $\Omega_{p2} > \Omega_{p1}$, and the corotation radius r_{c2} moves inward down to $(2 - 3) \cdot r_d$.

3.5 Models with the live halo

To analyse the influence of possible interior substructure in the dark matter, e.g. of presence of subhaloes predicted by the standard cosmology theory (Klypin et al. 1999; Bullock et al. 2001; Rocha et al. 2012), we ran our N-body simulations of interaction between the triaxial live halo and the stellar collisionless disc. We performed the simulations in several steps. First, we construct a quasi-steady triaxial live halo with a fixed stationary disc (a "frozen disc") inside. The halo is characterised by the parameter $\varepsilon \simeq 0.2 - 0.3$ as described before, which is initially assumed

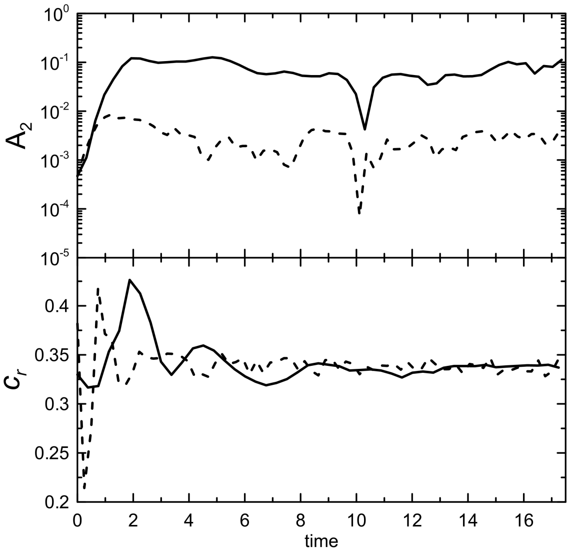

Figure 11. Comparison of the disc evolution in the models with live halo: the solid line is the case of a non-axisymmetric halo $\varepsilon = 0.1$, the dashed line is a case of symmetric halo $\varepsilon = 0$. Top panel: evolution of the Fourier harmonics $m = 2$. Bottom panel: evolution of the velocity dispersion.

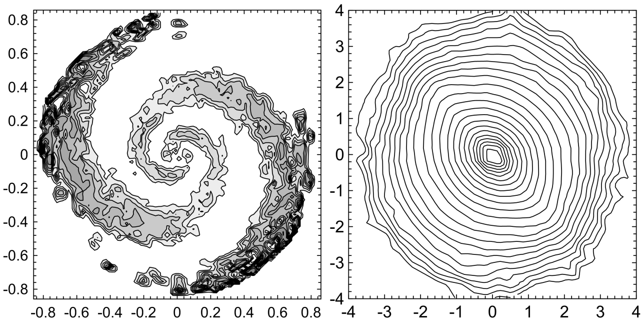

Figure 12. The spiral pattern (left) and the halo isodenses in projection to the disc's plane (right) in our model with the live halo.

to be constant along the radius. All disc particles were positioned within the radius $R_{opt} = 1.5$, and the halo particles were extended to $R_h = 5$. The total number of particles was $4 \cdot 10^6$ for the halo and $2 \cdot 10^6$ for the disc. The total halo mass in our modelling was $M_h = 4$. After several dynamical times the halo particles reached the state of relaxation and the initial numerical noise dissolved. Then we "unfreeze" the stellar disc particles instantly. Right after that, a two-arm spiral structure started forming, similar in its kinematics and morphological properties to that appeared in the case of rigid halo (see figure 12).

It is important to consider the effects of the stellar disc feedback on the dark halo shape in projection to the disc plane for a wide range of the non-axisymmetry parameter ε. In figure 12 we demonstrate the isodensity contours of the dark halo projected into the disc's plane at $t = 12$ (about 4 rotation periods at R_{opt}). We trace the evolution ε of the halo at three regions separately: 1) the central region $r_1 \leqslant r_d = 0.25$, 2) the disc periphery at $r_3 \geqslant 1$, and the intermediate region $r_1 < r < r_3$ (see figure 13). Up to time $t =$ 10, the amplitude of the spiral perturbations remains small and there is no noticeable stellar disc feedback on the halo shape. Some energy initially transfers from the triaxial halo particles to the disc, causing the spiral pattern generation. After that the central halo region becomes more axisymmetric, which means some energy is returned back to the halo due to the interaction with the spiral pattern. Local non-axisymmetric parameter in the intermediate zone also decreased down to $\simeq 0.15$. The influence of spiral waves on the halo shape in the outer region remains insignificant.

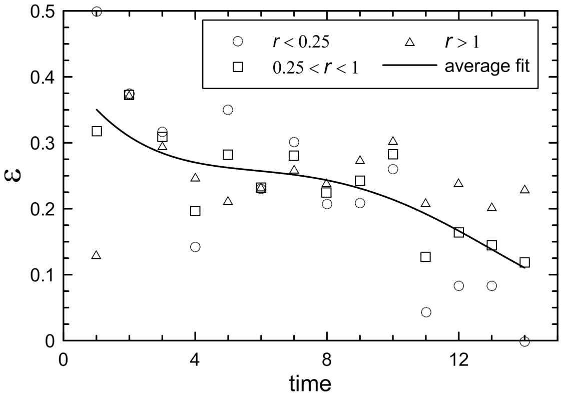

Figure 13. Evolution of the ε in the live halo at different radii. The line shows the best fitting for the central part of the disc.

We executed several simulations with live and symmetrical halo to investigate whether the disc and halo particle interactions can produce the disc heating. Such dynamical interaction could also generate some transient structures. Our modelling demonstrates the lack of the dynamical disc heating, at least in the marginally stable stellar disc in the presence of the live DM halo. In early moments of the modelling some oscillations of the disc velocity dispersion caused by relaxation of a small initial imbalance in particles distribution is observed (see the bottom panel in figure 11). After the relaxation is finished, the increasing of the velocity dispersion stops. Transient structures forming in the disc have an insignificant amplitude $< 1\%$ in the case of the symmetric halo (see e.g. top panel in figure 11). Note that its amplitude is several times larger than in the model with rigid halo model.

4 DISCUSSION

Cosmological simulations show that dark matter plays significant role in formation and evolution of galaxies of all morphological types. In this paper we consider a possibility of generation of a spiral pattern in the presence of non-axisymmetric dark halo.

The key question related to the spiral structure in the observed galaxies is whether the spirals are transient (Sellwood 2011) or long-lived features (Bertin and Lin 1996). In this paper we bring the existing evidences of non-spherical and, in general case, a triaxial dark matter distribution within and around the galaxies. Our numerical simulations suggest that the long-lived spiral patterns in stellar discs may be generated not only by the internal mechanisms (as it is traditionally assumed) but also via gravitational interaction between A triaxial dark halo and the galactic disc. Large-scale spirals emerge in our modelling even if the halo's triaxiality is as small as $\varepsilon \sim 0.02 - 0.05$. We demonstrate that mechanism of the long-lived spiral pattern formation discussed above acts very effectively even in dynamically hot stellar discs (initial value of the Toomre parameter $Q_T \sim 2 - 4$). Our preliminary simulations shows that the presence of a gaseous component does not change significantly this picture (Khoperskov et al. 2012). Note that similar mechanism can explain the existence of grand design spiral pattern observed in some dwarf early type galaxies (Jerjen et al. 2000; Lisker et al. 2006): we can assume that their spherical components are slightly triaxial.

We also infer that the halo axes orientation can be found from kinematic studies of the spiral pattern. As we showed above, the pattern angular velocity cannot be described by a single constant value, as in the classical axisymmetric models: at any radial distance it changes periodically twice for the period of rotation, as a result of nonaxisymmetry of the gravitational field of the halo (see figure 10). In principle, detailed measurements of the stellar velocity field can help detect the jumps of the phase velocity in the pattern (see figure 10), which spatially should point us at the major axis of the halo. The amplitude of the angular velocity perturbations can trace the deviation from the symmetry of the halo. The best candidates to this halo diagnostics are isolated non-barred spiral galaxies with small pitch angle of their spiral arms ($\leqslant 20^\circ$). Apparently the present day accuracy of the methods of the Ω_p estimation makes tracing its variation along the radial and azimuthal direction a difficult problem. Note however that there are some observational evidences of multiplicity of the pattern angular velocity in the inner and in the outer regions of galactic discs (see f.e. Buta and Zhang (2009)). A combined estimation of the bar pattern speed in the Milky Way obtained from the gas dynamics by Gerhard (2011) gives $\Omega_b \simeq 52 \pm 10$ km s^{-1} kpc^{-1} and places the corotation radius near the end of the bar at $3.5 - 5$ kpc). On the other hand, the Milky Way spiral arms rotate much slower: observations constrain the speed of the spiral pattern in the range of $\Omega_s \simeq 17 - 28$ km s^{-1} kpc^{-1} (Chakrabarty 2007), what corresponds to the corotation radius position near the solar neighborhood (~ 8 kpc). Thus, it is possible that the outer spiral structure in the Milky Way is relevant mostly to the triaxial halo-disc interaction, whereas the inner spiral arms are connected with the Milky Way bar.

We demonstrate in figure 13 how the dark matter halo becomes more spherical in the centre due to the spiral structure formation in the case of the initially triaxial halo. However, we bring detailed consideration of effects of the angular momentum feedback from the disc to the halo beyond the scope of this research. The dynamical interaction between the stellar disc and the DM halo occurs at resonances, and the result is the increasing of the halo rotation Athanassoula (2003). It is worth mentioning that the angular velocity of the bar in barred galaxies decreases in time due to dynamical frictions against the dark matter halo (see f.e. Debattista and Sellwood (2000)). Numerical cosmological simulations reveal the possibility of variations of the axes ratios in the galactic haloes during their evolution. Here we note that parallel to the secular processes (e.g. see Debattista et al. (2006)) the exchange by the angular momentum and energy between the live halo and density waves it creates may also lead to the quasi-stationary periodical variation of parameters of the spiral arms (including their pitch angle) with time. The latter, in turn, may cause a variation of the morphological type of a spiral galaxy during its evolution (see Mazzei and Curir (2003)).

5 CONCLUSIONS

We conducted high resolution N-body simulations to study interactions between the stellar disc and triaxial massive dark halo in terms of the spiral structure formation in disc for different initial disc and halo parameters. Our results are most relevant to the galaxies with mass-geometric properties similar to the Milky Way. The main conclusions are as follows:

1. A triaxial dark matter halo can produce and maintain a long-lasting (at least a few Gyr) grand design spiral structure in a stellar disc even if the disc is gravitationally stable.
2. As in the case of gaseous discs (see Khoperskov et al. (2012)), the stellar discs respond to the dark halo asymmetry via the global spiral pattern formation, even if triaxiality in the halo is rather small ($\varepsilon = 0.02 - 0.05$).
3. The resulting amplitude of the spiral waves ($m = 2$) depends on the triaxiality ε and is practically independent of the initial disc conditions.
4. Morphology of the spiral structure in our models is rather similar to that formed in classical density wave theory. The growing spiral pattern does not lead to significant redistribution of mass in the disc in the radial and azimuthal directions in the case of a non-axisymmetric massive halo.
5. Triaxial halo does not result to significant dynamic heating of the stellar disc (except, perhaps, the very initial stages of the interaction), in contrast to the case of a spiral pattern formed due to gravitational instability mechanisms.
6. Dynamics of the spiral pattern cannot be described by a single pattern angular velocity. Instead, we observe obviously two pattern angular velocities at any fixed radius. Most of the time the spiral pattern at given radius rotates slowly with the angular velocity Ω_{p1}, but twice for it rotation cycle its angular velocity jumps up to $\Omega_{p2} \simeq (4-5)\Omega_{p1}$ and then returns back. These jumps is caused by passing through the elongated potential well of the dark matter halo.
7. In general, morphology and kinematics of the spiral pattern in a stellar disc are quite similar to those obtained in modelling of gaseous discs embedded in non-axisymmetrical dark matter haloes (Bekki and Freeman 2002; Khoperskov et al. 2012).
8. There is a tendency for the halo to become more symmetric in the disc plane in the models that take into account self-consistent interaction between the disc and the dark halo. In this case a formation of spiral density waves remains effective in the outer regions of disc even when the inner regions of the halo have become axisymmetric.

6 ACKNOWLEDGMENTS

The authors would like to thank the anonymous referee for helpful comments and advises that improved the paper. Authors express their gratitude for valuable discussions to

V.I. Korchagin. This work was supported by grants RFBR (11-02-12247, 12-02-31452, 12-02-00685-a, 13-02-01251) and the Program for State Support for Leading Scientific Schools of the Russian Federation (grant NSh-3602.2012.2). This work was supported by the Federal Targeted Program of the Ministry of Education and Science of the Russian Federation "Research and Scientific-Pedagogical Personnel of Innovational Russia" for years 2009-2013. Numerical simulations were run on supercomputers of NIVC MSU "Lomonosov" and "Chebyshev". S. Khoperskov expresses his gratitude to non-commercial foundation "Dynasty" for financial support.

REFERENCES

Allgood B., Flores R.A., Primack J.R., Kravtsov A.V., Wechsler R.H., Faltenbacher A., Bullock J.S., 2006, MNRAS, 367, 1781

Athanasoula E., Bosma A., Papaioannou S., 1987, A&A, 179, 23

Athanassoula E., 2002, ApJ, 569, L83

Athanassoula E., 2003, MNRAS, 341, 1179

Bahcall J.N., 1984, ApJ, 276, 156

Bailin J., Steinmetz M., 2004, ApJ, 616, 27

Bailin J., Steinmetz M., ApJ, 2005, 627, 647

Barnes J., Hut P. 1986, Nature, 324, 446

Begeman K.G., Broeils A.H., Sanders R.H. 1991, MNRAS, 249, 523

Berentzen I., Shlosman I., 2006, ApJ, 637, 582

Berentzen I., Shlosman I., Jogee S. 2006, ApJ, 648, 807

Bershady M.A., Martinsson T.P.K., Verheijen M.A.W., Westfall K.B., Andersen D.R., Swaters R.A. 2011, ApJ, 739, 47

Bekki K., Freeman K.C., 2002, ApJ, 574, 21

Bertin G., Lin C.C., 1996, MA MIT Press, p. 271

Bett P., Eke V., Frenk C. S., Jenkins A., Helly J., Navarro J., 2007, MNRAS, 376, 215

Binney, J. & Tremaine, S., 2008, Galactic Dynamics. Princeton Univ. Press, Princeton, p.856

Bottema, R., 1993, A&A, 275, 16

Bryan S. E., Cress C. M., 2007, MNRAS, 380, 657

Burkert A., 1995, ApJL, 447, 25

Buta R.J., Zhang X., 2009, ApJ, 182, 559

Bizyaev D., Mitronova S., 2002, A&A, 389, 759

Bizyaev D., Mitronova S., 2009, ApJ, 702, 1567

Bullock J.S., Kolatt T.S., Sigad, Y., Somerville R.S., Kravtsov A.V., Klypin A.A., Primack J.R., Dekel A., 2001, MNRAS, 321, 559

Ceverino D., Klypin A. 2007, MNRAS, 379, 1155

Chakrabarty, D. 2007, A&A, 145, 162

Combes F., 2006, EAS Publ. Ser., 20, 97

Cooper A.P., Cole S., Frenk C.S., White S.D.M., Helly J., Benson A.J., De Lucia G., Helmi A., Jenkins A., Navarro J.F., Springel V., Wang J., 2010, MNRAS, 406, 744

De Simone R., Wu X., Tremaine S., 2004, MNRAS, 350, 627

Debattista V.P., Sellwood J.A., 2000, ApJ, 543, 704

Debattista V.P., Mayer L., Carollo C.M., Moore B., Wadsley J., Quinn T., 2006, ApJ, 645, 209

Debattista V.P., Moore B. Quinn T., Kazantzidis S., Maas R., Mayer L., Read J., Stadel J., 2008, ApJ, 681, 1076

Diemand J., Kuhlen M., Madau P., 2007, ApJ, 657, 262

Diemand J., Moore B., 2011, Advanced Science Letters, 4, 297

Dubinski J, Chakrabarty D., 2009, ApJ, 703, 2068

Dubinski J., Berentzen I., Shlosman I., 2009, ApJ, 697, 293

Einasto J., 1965, Trudy Inst. Astrofiz. Alma-Ata, 51, 87

El-Zant A.A., Habler B., 1998, New Astronomy, 3, 493

Fux R., 1997, A&A, 327, 983

Fellhauer M., Belokurov V., Evans N. W., Wilkinson M. I., Zucker D. B., Gilmore G., Irwin M. J., Bramich D. M., Vidrih S., Wyse R. F. G., Beers T. C., Brinkmann J., 2006, ApJ, 651, 167

Garbari S., Read J.I., Lake G., 2011, MNRAS, 416, 2318

Gentile G., Burkert A., Salucci P., Klein U., Walter F., 2005, ApJ, 634, 145

Gerhard O., 2011, Mem. S.A.It., 18, 183

Griv E., Gedalin M., 2004, AJ, 128, 1965

Gustafsson M., FairBairn M., Sommer-Larsen J., 2006, Phys. Rev. D 74, 123522

Hayashi E., Navarro J.F., 2006, MNRAS, 373, 1117

Hayashi E., Navarro J.F., Springel V., 2007, MNRAS, 377, 50

Heller C.H., Shlosman I., Athanassoula E., 2007, ApJ, 671, 226

Helmi A., 2004, MNRAS, 351, 643

Ibata R., Lewis G.F., Irwin M., Totten E., Quinn T., 2001, ApJ, 551, 294

Ideta M., Hozumi S., 2000, ApJ, 535L, 91

Iodice E., Arnaboldi M., Bournaud F., Combes F., Sparke L.S., van Driel W., Capaccioli M., 2003, ApJ, 585, 730

Jerjen H., Kalnajs A., Binggeli B., 2000, A&A, 358, 845

Just A., Jahrei H., 2010, MNRAS, 402, 461

Kazantzidis S., Abadi M.G., Navarro J.F., 2010, ApJ, 720L, 62

Keller S. C., Murphy S., Prior S., Da Costa G., Schmidt B., 2008, ApJ, 678, 851

Khoperskov A.V., Zasov A.V., Tyurina N.V., 2003, ARep, 47, 357

Khoperskov S.A., Shustov B.M., Khoperskov A.V., 2012, ARep, 56, 664

Khoperskov A.V., Zasov A.V., Tiurina N.V., 2003, ARep, 47, 357

Khoperskov A.V., Eremin M.A., Khoperskov S.A., Butenko M.A., Morozov A.G., 2012, ARep, 56, 16

Khoperskov A.V., Bizyaev D., Tyurina N.V., Butenko M., 2010, Astron. Nachr., 331, 731

Klypin A., Kravtsov A.V., Valenzuela O., Prada F., 1999, ApJ, 522, 82

Klypin A.A., Trujillo-Gomez S., Primack J., 2011, ApJ, 740, 102

Koopmans L.V.E., de Bruyn A.G., Jackson N., 1998, MNRAS, 295, 534

Korchagin V., Kikuchi N., Miyama S.M., Orlova N., Peterson B.A., 2000, ApJ, 541, 565

Korchagin V.I., Girard T.M., Borkova T.V., Dinescu D.I., van Altena W.F., 2003, AJ, 126, 2896

Kuhlen M., Diemand J., & Madau P., 2007, ApJ, 671, 1135

Law D.R., Majewski S.R., Johnston K.V., 2009, ApJ, 703, 67

Lisker T., Grebel E.K., Binggeli B., 2006, AJ, 132, 497

Lynden-Bell D., Ostriker J.P., 1967, MNRAS, 136, 293

Macciò A. V., Dutton A.A., van den Bosch F.C., Moore B., Potter D., Stadel J., 2007, MNRAS, 378, 55

Macciò A. V., Stinson G., Brook C. B., Wadsley J., Couchman H. M. P., Shen S., Gibson B. K., Quinn T., 2012, ApJ, 744, L9

Machado R.E.G., Athanassoula E., 2010, MNRAS, 406, 2386

Maller A.H., Simard L. Guhathakurta P., Hjorth J., Jaunsen A.O., Flores R.A., Primack J.R., 2000, ApJ, 533, 194

Mazzei P., Curir A., 2003, ApJ, 591, 784

Masset F.S., Bureau M., 2003, ApJ, 586, 152

Morrison H., Helmi A., Sun J., Liu P., et al., 2009, ApJ, 694, 130

Muñoz-Cuartas J.C., Macciò A.V., Gottlöber S., Dutton A.A., 2011, MNRAS, 411, 584

Navarro J.F., Frenk C.S., White S., 1997, ApJ, 490, 493

Navarro J.F., Ludlow A., Springel V., Wang J., Vogelsberger M., White S.D.M., Jenkins A., Frenk C.S., Helmi A., 2010, MNRAS, 402, 21

Newberg H.J., Yanny B., Cole N., 2007, ApJ, 668, 221

Oguri M., Lee J., Suto Y., 2003, ApJ, 599, 7

Reshetnikov V.P., Sotnikova N.Ya., 2000, Astron. Lett., 26, 277

Rocha M., Peter A.H.G., Bullock J.S., Kaplinghat M., Garrison-Kimmel S., Onorbe J, Moustakas L.A., 2012, arXiv:1208.3025v1

Romano-Diaz E., Shlosman I., Heller C., Hoffman Y., 2008, ApJ, 687, 13

Roskar R., Debattista V.P., Brooks A.M., Quinn T.R., Brook C.B., Governato F., Dalcanton J.J., Wadsley J., 2010, MNRAS, 408, 783

Ryden B.S., 2006, ApJ, 641, 773

Saburova A.S., Zasov A.V., 2012, Astron. Letters, 38, 139

Sackett P.D., Sparke L.S., 1990, ApJ, 361, 408

Sackett P.D., Rix H.-W., Jarvis B.J., Freeman K.C., 1994, ApJ, 436, 629

Sackett P.D., Pogge R.W., 1995, AIP Conf. Proc., 336, 141

Safronov V. S., 1960, Ann. d'Astrophysique, 23, 979

Sellwood J., 2011, MNRAS, 410, 1637

Sesar B., Juric M., Ivezic Z., 2011, ApJ, 731, 4

Sotnikova N.Ya., Rodionov S.A., 2005, Astr. Letter., 31, 15

Tinker J.L., Ryden B.S. 2002, arXiv:astro-ph/0209165

Toomre A., 1964, ApJ, 139, 1217

Tutukov A.V., Fedorova A.V., 2006, ARep., 50, 785

Vivas A.K., Zinn R., Gallart C., 2005, AJ, 129, 189

Vitvitska M., Klypin A.A., Kravtsov A.V., Wechsler R.H., Primack J.R., Bullock J.S., 2002, ApJ, 581, 799

Whitmore B.C., McElroyD.B., Schweizer F., 1987, ApJ, 314, 439

Westfall K. B., Bershady M. A., Verheijen M. A. W., Andersen D. R., Martinsson T.P.K, Swaters R. A., Schechtman-Rook A., 2011, ApJ, 742, 18

Widrow L.M., 2008, ApJ, 679, 1232

Zasov A.V., Makarov D.I., Mikhailova E.A., 1991, PAZh, 1991, 17, 884

Zasov A.V., Bizyaev D.V., Makarov D.I., Tyurina N.V., 2002, Astr. Lett, 28,527

Zasov A.V., Khoperskov A.V., Tiurina N.V., 2004, Astr. Lett., 30, 593

Zentner A. R., Kravtsov A. V., Gnedin O. Y., Klypin A. A., 2005, ApJ, 629, 219

Zibetti S., White S., Brinkmann J., 2004, MNRAS, 347, 556

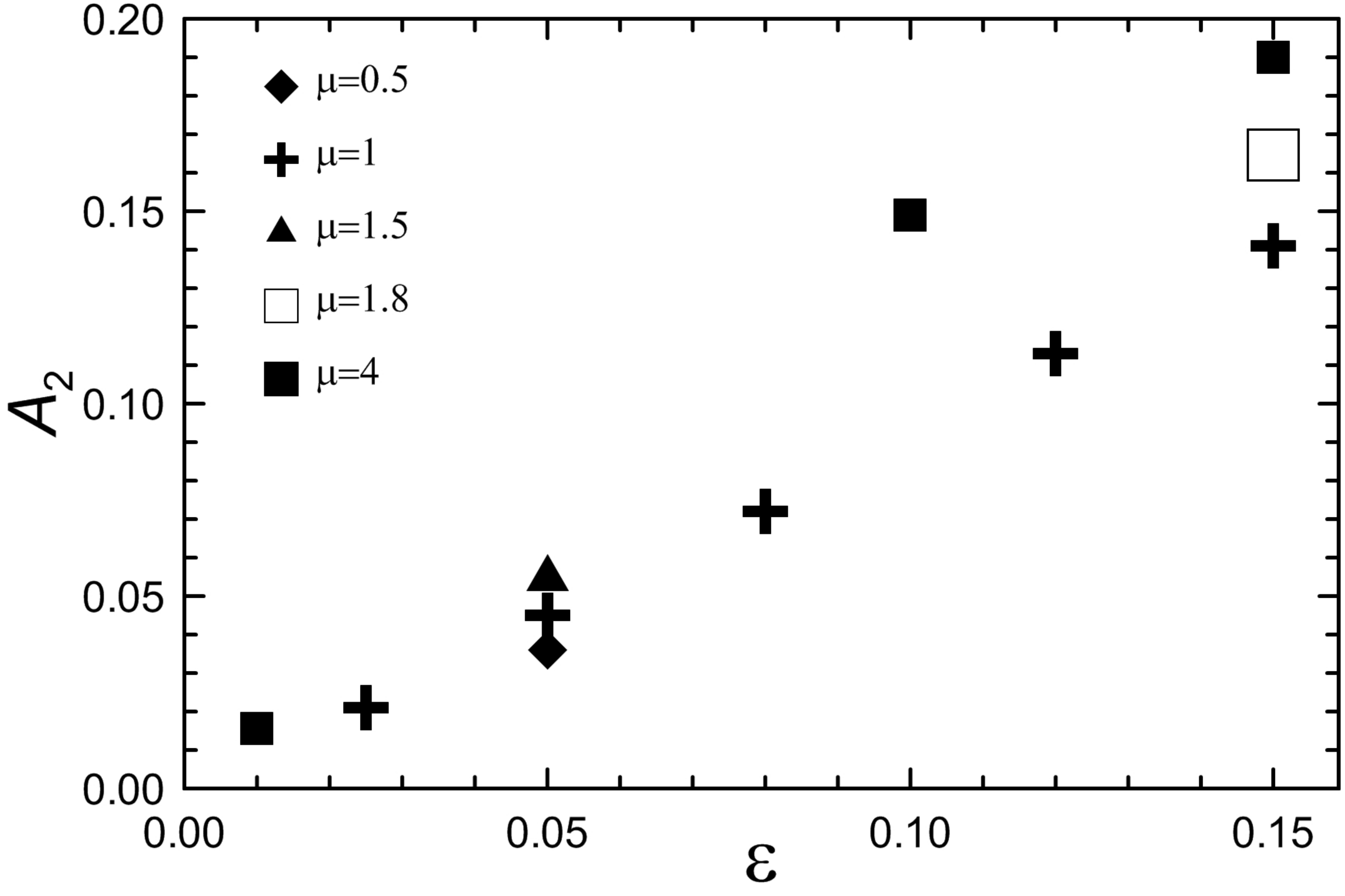

A2
0.00
0.05
0.10
0.15
0.20
0.00
0.05
0.10
0.15
ε
μ=0.5
μ=1
μ=1.5
μ=1.8
μ=4